Research Article | Vol. 29, No. 14 / 5 July 2021 / Optics Express 22117
Optics EXPRESS

Agile spectral tuning of high order harmonics by interference of two driving pulses

VITTORIA SCHUSTER,[1,*] VINZENZ HILBERT,[1] ROBERT KLAS,[1,2] CHANG LIU,[1,2] MAXIM TSCHERNAJEW,[3] BIRGITTA BERNHARDT,[4] JAN ROTHHARDT,[1,2,5] AND JENS LIMPERT[1,2,5]

[1]*Institute of Applied Physics, Friedrich-Schiller University Jena, D-07745 Jena, Germany*
[2]*Helmholtz-Institute Jena, D-07743 Jena, Germany*
[3]*Active Fiber Systems GmbH, D-07745 Jena, Germany*
[4]*Institute of Experimental Physics & Institute of Material Physics, Graz University of Technology, 8010 Graz, Austria*
[5]*Fraunhofer Institute of Applied Optics and Precision Engineering, D-07745 Jena, Germany*
[*]*vittoria.schuster@uni-jena.de*

Abstract: In this work, the experimental realization of a tunable high photon flux extreme ultraviolet light source is presented. This is enabled by high harmonic generation of two temporally delayed driving pulses with a wavelength of 1030 nm, resulting in a tuning range of 0.8 eV at the 19th harmonic at 22.8 eV. The implemented approach allows for fast tuning of the spectrum, is highly flexible and is scalable towards full spectral coverage at higher photon energies.

1. Introduction

Over the past three decades high harmonic generation (HHG) of ultrashort driving laser pulses has emerged as a complimentary technique to large-scale facilities for the generation of extreme ultraviolet (XUV) light. The broad spectral coverage of the harmonic comb, coherence and ultrashort pulse duration (fs - as) [1], achievable with HHG have enabled a large variety of table-top applications. These range from imaging experiments with extreme spatial resolution [2] to XUV spectroscopy, which gives access to the electronic structure of atoms, ions, molecules and solids [3–12]. Often, selecting one narrow bandwidth single harmonic line with a high photon flux is beneficial for such experiments. However, the discrete orders of the harmonic comb, which are odd multiples of the driving laser frequency, can constitute a severe limitation for these experiments. Tunable HHG sources can increase the spectral coverage while maintaining a narrow linewidth and high flux, thus enabling to target specific resonances regardless of their spectral position. This holds immense potential for aforementioned spectroscopic techniques and has been employed for the generation of quasi-supercontinua [13]. Furthermore, tunable XUV sources are of great interest for lensless XUV multispectral imaging. Here, scanning the light source over a characteristic resonance of the sample provides access to spectral information [14], which otherwise needs to be retrieved from broadband measurements with larger computational [15–18], or experimental effort [19–21].

A large variety of spectrally tunable HHG sources have been demonstrated, often relying on manipulation of the driving laser field. Most intuitively, spectrally tunable infrared sources have been employed, either by high-order frequency mixing the weak but tunable output of an optical parametric generator with a fixed-frequency high pulse energy laser inside the gas target [22,23], by directly driving the HHG process with a tunable optical parametric amplifier (OPA) output [13,24,25], or by tuning the fundamental through soliton dynamics [26]. Other approaches

#424024 https://doi.org/10.1364/OE.424024
Journal © 2021 Received 2 Mar 2021; revised 18 Apr 2021; accepted 6 May 2021; published 29 Jun 2021

Optics EXPRESS

exploit the HHG spectrum's dependence on the driving laser intensity through blue-shifting [27], on the pulse chirp [28], or both [29], sometimes in combination with chromatic focusing [30]. Furthermore, the emergence of devices for tailored modification of the spectral phase and amplitude of the driving laser has led to general flexibility in the custom control of HHG spectra [31–33].

Despite the numerous implementations, the demand for efficient tunable HHG sources with low complexity, both with regards to the setup and the optimization parameters, remains unabated. Oldal et al. [34] recently presented theoretical considerations and simulation results for a tunable high-harmonic generation source that relies solely on the time delay between two identical driving pulses of fixed wavelength to shift the HHG spectrum. An implementation of this approach at existing HHG sources is possible without modification to the driving laser, promising an accessible route to tuning narrowband XUV spectra. It provides a high tuning speed, is compatible with small pulse energies and scalable to high average powers and broad driving laser spectra. This constitutes a valuable addition to the parameter space covered by the previously given examples, enlarging the possible range of experimental implementations. In this work we present the first experimental demonstration of a tunable HHG source following the two-pulse method proposed in Ref. [34].

2. Theoretical background

The approach is based on shifting the central photon energy E_{fund} of the fundamental driving pulse, which translates to a change in photon energy of the generated XUV radiation. The central wavelength of the fundamental beam is tuned solely by exploiting the spectral interference of two identical delayed pulses of constant spectrum. Figure 1(a) shows spectra of a thus composed double pulse for several delays. For a given path delay d, different wavelength components λ of the spectrum interfere differently, since the introduced phase shift is given by $\varphi = 2\pi d/\lambda$. The resulting spectral fringe pattern changes in position and width as the delay between the pulses is tuned. When considering delay variations smaller than the central wavelength of the individual pulses, the main effect lies in the change of position of the fringe pattern. As is illustrated in Fig. 1(a), for increasing delay the fringe pattern is shifted from shorter to longer wavelengths. For sufficiently wide fringes, here corresponding to delays around 14 times the central wavelength of a single pulse λ_{c1}, broad portions of the spectrum interfere destructively. These components do not contribute to the resulting composite pulse and its mean wavelength λ_{c2}. This results in a continuous increase of the central wavelength over the constructive part of the interference cycle (see delays between 13.8 λ_{c1} and 14.2 λ_{c1} in Fig. 1(a)). When analyzing delay variations larger than λ_{c1}, the changes in width of the fringe pattern become more apparent. As can be seen in Fig. 1(b), in the constructive part of each interference cycle (highlighted in light red), the central wavelength of the composite pulse increases with the delay, while in the destructive part it decreases. However, due to the changing fringe width, both the intensity and spectral tuning range are different for each interference cycle. Thus, the choice of an appropriate delay enables controling the composite pulse's central energy and additionally permits to influence its intensity.

In a first approximation, the photon energy of the high-order harmonic of order H driven by a fundamental field with central photon energy E_{fund} can be expressed as $H \cdot E_{\mathrm{fund}}$. Thus, by changing the central energy of the fundamental by ΔE_{fund}, the central energy of the harmonic changes by ΔE_{H}:

$$E_{\mathrm{H}} = H \cdot E_{\mathrm{fund}} \Rightarrow \Delta E_{\mathrm{H}} = H \cdot \Delta E_{\mathrm{fund}}$$

This simplified spectral picture neglects the temporal structure of the driving pulse and the HHG process. It is, however, a good approximation under the assumption that the temporal portions of the composite pulse with the highest intensity contribute dominantly to its central wavelength and that phase matching is optimized for them to generate the largest part of the XUV flux. This is often favorable in the experiment due to the increased single-atom response of the

Optics EXPRESS

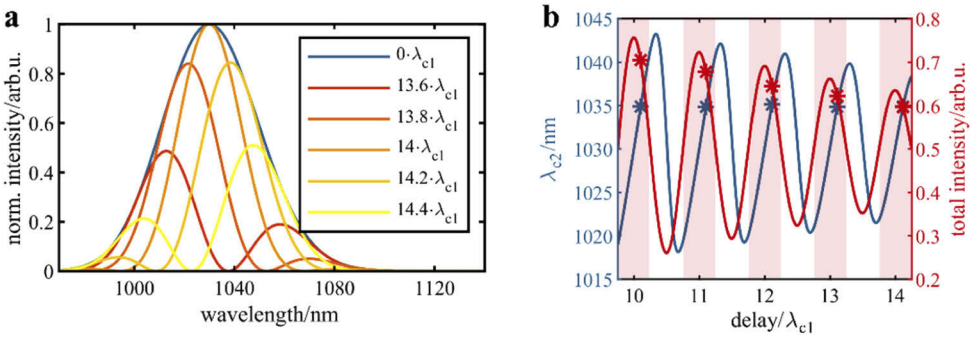

Fig. 1. Simulation of tuning the composite pulse spectrum through the delay. **a**: Simulated spectra of a composite pulse for different delays between the individual pulses, given in multiples of the central wavelength of a single pulse λ_{c1}, 1030 nm. The blue curve depicts the spectrum for zero path delay, which is analogous to the spectrum of the individual pulses. **b**: Delay tuning over more than one interference cycle. The central wavelength of the composite pulse λ_{c2} and its total intensity are plotted over the delay given in central wavelengths of a single pulse λ_{c1}. The constructively interfering delay ranges around multiples of λ_{c1} are highlighted in light red. Due to the constructive and destructive interference of different portions of the spectrum, the central wavelength and total intensity of the composite pulse change with varying delay. The asterisks mark the values at constructive delays for which λ_{c2} is 1035 nm. The spectra are calculated through Fourier transformation of the temporal composite pulses. The Fourier-limited duration of the individual pulses is 35 fs. For details on the temporal structure of composite pulses see Ref. [34].

generating medium for higher intensities [35]. As can be seen in Fig. 1, the different interference conditions that are created by changing the delay do not only influence the composite pulse spectrum, but also its intensity. Consequently, the generating conditions of the XUV light vary for different delays and some level of adjustment is necessary to ensure efficient high-harmonic generation for a large delay range. While higher intensities are favorable for the single-atom response of the generating medium ($\propto I^9$ [35]), they do not necessarily lead to a larger XUV flux due to phase-matching effects. Especially the increase of the ionization fraction above the critical ionization, beyond which true phase-matched HHG is not possible [36], limits the driving laser intensity for a given pulse duration. While phase matching is influenced by many parameters, such as focusing geometry, aperture of an iris in the fundamental laser beam, gas pressure and target position, these are in the following kept constant within one measurement for the sake of experimental simplicity and comparability.

3. Experimental setup

In this experiment, the driving double pulse is composed of two time-delayed pulses of equal energy and duration by a passively stable Michelson-type interferometer. This approach allows for continuous tuning over a large delay range and only utilizes elemental optical components which support scaling to high power and broad spectral bandwidth. Furthermore, minimizing the nonlinear effects occurring in solid optical materials results in a highly flexible setup that is directly implementable at the output of systems with short pulses and high average powers.

A schematic of the setup is depicted in Fig. 2. The output of a commercial pulsed 35 fs, 200 kHz Yb fiber amplifier system emitting at 1030 nm and including a hollow core fiber compression stage is split into two partial beams with pulse energies of 37 µJ each by an intensity beam splitter. A closed-loop high-precision translation stage in one of the interferometer arms allows for continuous control of the relative delay between the two partial beams, which are

Optics EXPRESS

superimposed again at a second beam splitter. The spectrum of the resulting combined beam is monitored through a mirror leak with an optical spectrum analyzer. The beam itself passes through an iris aperture transmitting 95% of its power before entering a vacuum chamber. Here, it is focused using a lens of 100 mm focal length to a waist radius of 13 µm into a 70 µm diameter Krypton gas jet with a backing pressure of 5 to 5.5 bar to generate the harmonics. The resulting XUV light is separated from the driving infrared laser by two grazing-incidence plates [37] and a 200 nm Al foil and consequently analyzed with a flat-field grating spectrometer that provides spectral and spatial information on the XUV beam. By using the known distance of the focal spot to the spectrometer detector the XUV beam divergence can be estimated. The HHG process is optimized for the 19th harmonic (H19). Since the tuning ranges of H17 and H21 partially lie within the recorded spectral range, they could be evaluated where fitting.

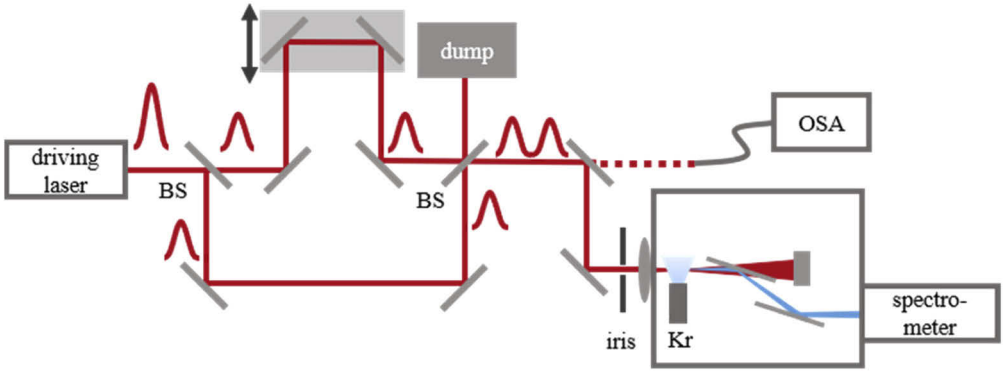

Fig. 2. Schematic of the setup for tunable high-harmonic generation. BS: beam splitter; OSA: optical spectrum analyzer. Kr: Krypton gas-jet.

4. Results

4.1. Continuous and fast spectral tuning

The highest tuning speed for the XUV spectrum can be achieved by continuously driving the delay over the constructive part of a single fundamental interference cycle, while keeping the remaining HHG optimization parameters constant (i.e. backing pressure, iris diameter, jet position and focusing geometry). To maintain a high photon flux over the full tuning range, the fundamental intensity should remain steady as well. While the occurrence of intensity variations is inevitable due to the interferometric nature of the tuning process, their amplitude can be limited through the choice of the utilized interference cycle. As can be seen in Fig. 1(b), the intensity variation as well as the spectral tuning range decrease for increasing delay. This results in a tradeoff between the spectral tuning range and the intensity stability. For the parameters used in this work, the optimal delay range is around the constructive interference at $14\lambda_{c1}$ (λ_{c1}=1030 nm) and was utilised for the measurements depicted in Fig. 3.

The spectra shown in Fig. 3(a) and Fig. 3(b) are acquired while continuously decreasing the delay between the two pulses over slightly more than one driving laser cycle at a speed of 0.1 µm/s. The infrared data is subsequently post-processed to remove uncompressed components that do not contribute to HHG by suppressing the spectral segment around 1030 nm that has not undergone spectral broadening by the hollow core stage. It can be seen in Fig. 3(a) that the centers of both the driving and the XUV spectrum shift from smaller to bigger photon energies over the constructively interfering part of the cycle. Since the depicted delay range is 14 driving laser wavelengths away from zero path delay, the driving pulses do not completely cancel each

Optics EXPRESS

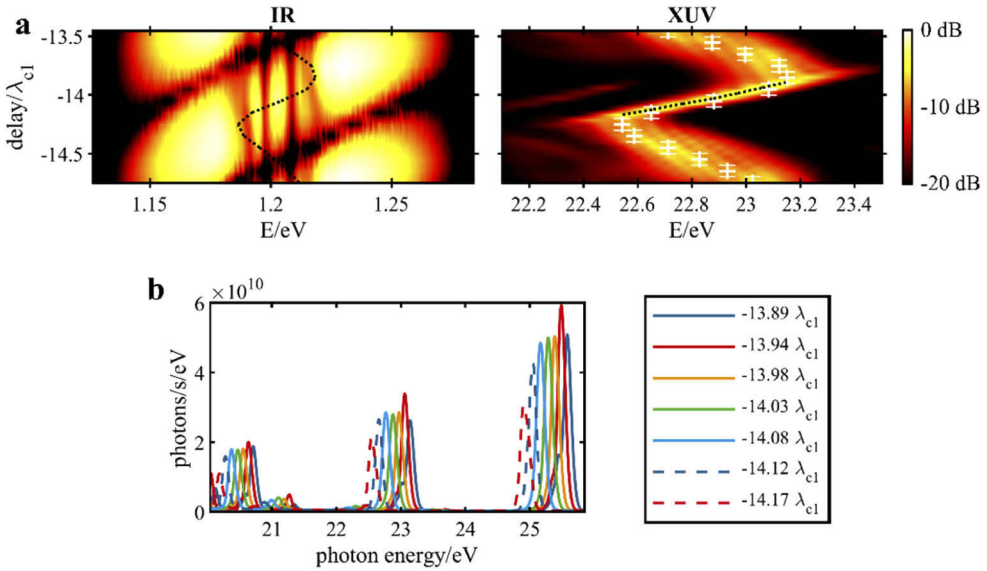

Fig. 3. Tuning of H19 by solely changing the delay between the driving pulse pair. a: Post-processed spectra of the driving composite pulse (left) and H19 (right) over a delay range of more than one driving laser cycle. The black dotted line in the left plot marks the central photon energy of the composite pulse. White crosses in the right plot represent the central photon energy of the driving composite pulse multiplied with the harmonic order 19. The error bars refer to the matching precision of the simultaneously acquired XUV and infrared traces. The peak photon energy of H19 is marked by a black dotted line in the right plot for constructive delays. b: XUV spectra of H17-H21 between delays of $-13.89\ \lambda_{c1}$ and $-14.17\ \lambda_{c1}$.

other around the point of destructive interference (see also Fig. 1(b)). Therefore, a weaker and broader harmonic line shifting back to smaller photon energies is produced in this delay range.

The scanning speed and the spacing between the measurements in Fig. 3 are solely limited by the acquisition speed of the spectrometers. Without any further adjustment of the HHG parameters or iris aperture, the spectrum of the 19th harmonic is tuned over 0.6 eV in three seconds, with just 14% relative standard deviation of the peak flux. Moreover, the spectral bandwidth maintains a relative standard deviation of 4% and the XUV beam divergence of 15% over this tuning range. This constitutes a remarkable ease and speed of tuning the spectral position of the high harmonic, while maintaining notable constancy of the other mentioned parameters, the values of which are marked as red dots in Fig. 4.

The interferometer stability is important for successful long-term measurements and in this experiment care was taken to realize a passively stable setup. Slow drifts can be neglected in the presented measurements, since their acquisition was performed while actively changing the delay between the two pulses at 0.1 µm/s. Fast vibrations can be estimated to be below 50 nm, since the spectral positions of the harmonic lines can be clearly distinguished for successive measurements in Fig. 3(b). This would be hindered by delay jitters with higher amplitudes than the delay spacing occurring during the integration time of the spectrometer, 0.1 s.

4.2. *Extended tuning range*

While the approach explained above offers the fastest tuning speed, the spectral tuning range over which a constant XUV flux is maintained can be extended further. This requires additional optimization of the phase matching conditions, which can be achieved by solely adjusting the

Optics EXPRESS

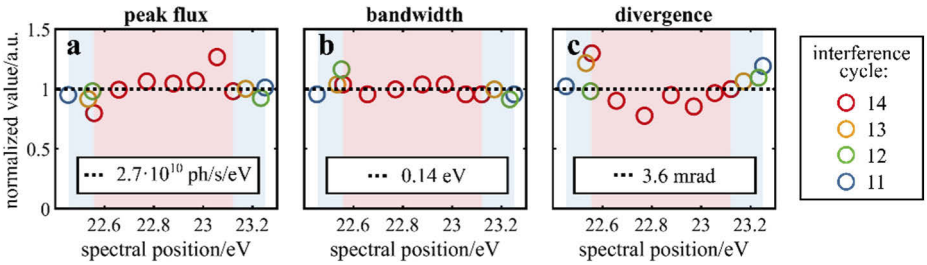

Fig. 4. Parameters of H19 for delays in different interference cycles. a: peak flux. b: FWHM spectral bandwidth. c: XUV beam divergence. The colors of the dots represent the interference cycles the measurements are acquired in (closest multiple of λ_{c1}). The light red shading visualizes the tuning range achieved for continuous fast tuning around 14 λ_{c1} and the blue shading the full tuning range for all utilized delays. All parameters are normalized to their respective average, which is given in the inset.

fundamental intensity. The other optimization parameters (i.e. backing pressure, jet position and focusing geometry) are kept constant, ensuring a simple setup as well as a moderate tuning speed.

Using this, a broader tuning range can be accomplished in two different manners. When regarding only one interference cycle, the delays with maximal spectral shift correspond to smaller intensities as larger portions of the spectrum interfere destructively. This could be addressed by optimizing the HHG parameters for large spectral shifts and, in between tuning steps, reducing the intensity at more constructive interference (e.g. by decreasing the HHG iris diameter). This would, however, necessitate the control of an additional parameter besides the delay, reducing the agility of the method for the presented realization.

As the strength of the setup utilized in this work lies in the fast control of the delay, a different approach is chosen, the basis of which is utilizing a delay range that extends over more than one interference cycle. When regarding the delay range depicted in Fig. 1(b), it can be seen that for a given central wavelength of the composite pulse the intensity is smaller for larger delays. This can be exploited by optimizing the phase matching parameters for moderate intensities and choosing the delay that provides the most similar fundamental intensity at the desired spectral position.

The increase of the covered spectral range with regard to the results displayed in Fig. 3 is achieved solely by extending the utilized delay range from the 14th to the 11th interference cycle. All further parameters remain unchanged. The results for the increased tuning range of H19 are depicted in Fig. 4. The values of the continuously tuned spectra are represented by red dots. By including further interference cycles, the central energy of H19 is tuned over a range of $\Delta E_{XUV,max}$ =0.8 eV, extending the tuning range by 33%. The relative standard deviation of the peak flux is kept at 11% and of the bandwidth at 6% and of the beam divergence at 15%. The resulting spectral coverage with respect to the spacing between adjacent harmonic lines is 33% for H19.

Some rough trends can be seen across the spectral tuning range in Fig. 4, which can be interpreted, in a simplified approach, through the fundamental intensity. Spectra with smaller spectral shift tend to occur at delays at which larger portions of the IR spectrum interfere constructively. The higher resulting intensity enables efficient HHG in a larger volume, thus decreasing the divergence of the XUV light (Fig. 4(c)). The opposite tendency can be observed for increasing spectral shifts. The intensity picture can also be used to interpret why the less shifted spectra are recorded for interference cycles corresponding to larger delays. As depicted in Fig. 1(b), the peak intensity of each interference cycle, which occurs at multiples of λ_{c1}, decreases with increasing delay. Thus, phase matched high harmonics can be generated with

Optics EXPRESS

the less spectrally shifted fundamental despite the constructive interference of large parts of the spectrum.

As mentioned above, the trends across the values displayed in Fig. 4 are simplified and specific to the parameters of the experiment. However, their low variation promises a good compatibility of the interferometric spectral tuning method with other approaches to the optimisation of the phase matching process, e.g. through the iris opening, backing pressure or gas jet position.

4.3. Scaling to full spectral coverage

In the following, we will discuss paths to increase the tuning range towards complete spectral coverage. The maximum achievable spectral tuning range of the XUV light depends mainly on two parameters: the harmonic order and the spectral bandwidth of the driving laser.

To illustrate the influence of the harmonic order, the spectral position of multiple harmonics is evaluated for two delays. Namely, 7.9 µm and 8.3 µm, are chosen such that H17, H19 and H21 are all within the spectral range covered by the spectrometer detector and furthermore the second diffraction orders of H35 and H37 are clearly visible. The diffraction angle for the second order is equivalent to the first order of light having half its photon energy. Consequently, in the right panel of Fig. 5(a) H35 and H37 appear between H17 and H19, although very weakly due to the reduced diffraction efficiency of the grating. The relation between the spectral shift of the harmonic lines and the delay shows a nonlinearity in Fig. 5(a) (right panel). This can be attributed to the nonlinearity of both the central photon energy, indicated by black dots in the left panel of Fig. 5(a), and the intensity of the composite pulse with regard to the delay. The high driving laser intensity can lead to the occurrence of blue shift at the delays with more constructive IR interference. For a sufficient approximation, the two evaluated delays are considered to be free from this blue shift and all harmonic lines are assumed to be generated at the same emission times, and thus equal instantaneous wavelength of the driving composite pulse. The resulting measured tuning ranges of the different harmonic orders are plotted in Fig. 5(b). As derived above, the relationship between the tuning range of a harmonic ΔE_{H} and its order H should be linear. The slope of the resulting linear fit matches the tuning range of the fundamental central energy, 0.03 eV per harmonic order.

Assuming the maximum tuning range of the fundamental $\Delta E_{\mathrm{fund,max}}$ to be proportional to the full width at half maximum frequency bandwidth BW, leads to the following relation for Fourier limited individual pulses of duration τ_{fund}:

$$\Delta E_{\mathrm{fund,\,max}} \propto BW \propto 1/\tau_{\mathrm{fund}}$$

$$\Rightarrow \Delta E_{\mathrm{XUV,max}} = H \cdot \Delta E_{\mathrm{fund,max}} \propto H/\tau_{\mathrm{fund}}$$

An estimation of the achievable spectral coverage based on this relation and the results depicted in Fig. 4 is shown in Fig. 5(c). The dark blue area marks parameter combinations with complete spectral coverage. For the implemented pulse duration of 35 fs and 1.03 µm driving laser wavelength, gap-free spectral tuning is expected for harmonic orders larger than 55 (photon energy > 66 eV). This can be extended by using shorter pulses or larger wavelengths λ_{fund}. For a given pulse duration, the minimal harmonic order for continuous tuning H_{min} scales with $1/\lambda_{\mathrm{fund}}$, roughly halving H_{min} for 2 µm drivers, and doubling it for 0.5 µm in relation to the value derived from Fig. 5(c).

One advantage of the interferometric tuning approach used in this experiment is that no part of the driving laser power is lost a priori. If no change of the central energy is needed, the relative delay can be set to zero. In this case the interference of the two pulses is fully constructive and the full power of the fundamental laser used for HHG. Indeed, similar XUV spectra and efficiencies have been achieved by bypassing the interferometer, thus using a single driving pulse with the same overall pulse energy. Switching between using the full IR spectrum or parts of it is

Optics EXPRESS

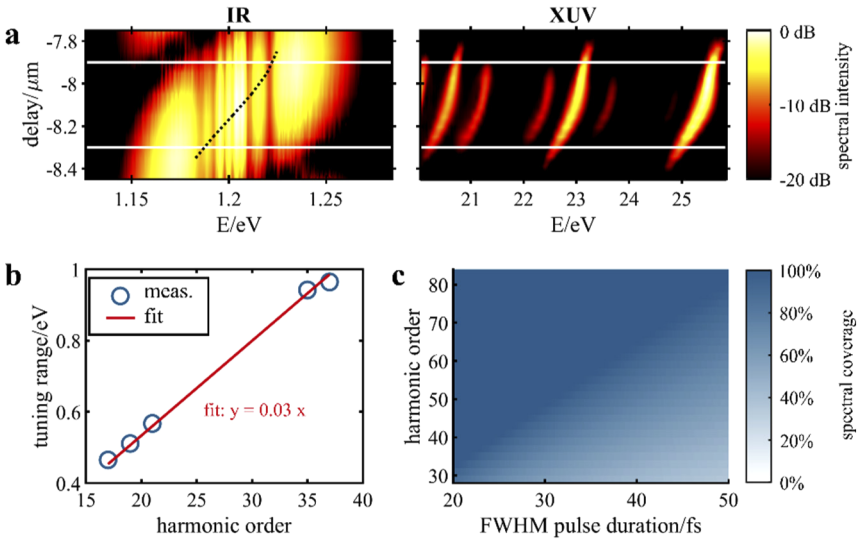

Fig. 5. Scaling of the tuning range. a: Post-processed spectra of the driving composite pulse (left) and resulting XUV spectra (right). The white lines mark the delays evaluated in b. The dotted black line marks the central photon energy of the composite pulse b: Evaluation of the spectral tuning rages of the peaks of H17-21, H35 and H37 between the delays of −8.3 µm and −7.9 µm. The red line shows a linear fit to the data, in good agreement with the expected slope, 0.03 eV/HH order. c: Predicted dependence of the XUV spectral coverage on the Fourier-limited duration of the individual pulses at 1030 nm and the harmonic order.

possible by changing just one parameter: the delay. This underlines the efficiency and versatility of the interferometric approach.

5. Conclusion

In conclusion, we demonstrate an efficient, fast spectrally tunable HHG source driven by time-delayed composite pulses. The narrowband 19th harmonic of a 1030 nm driving laser is shown to be tunable from 22.3 eV to 23.1 eV for the laser parameters utilized in this work. The development potential to full spectral coverage is discussed. This work opens numerous possibilities to tailor this tuning technique to different requirements. The employed Michelson-type interferometer can easily be modified to support a wide range of driving laser parameters and does not rely on prior adjustment of the pulse properties. Due to these qualities, it is outstandingly suitable for commercial driving lasers or user facilities with limited beam time. Since only highly reflective mirrors and a beam splitter are required, it is power scalable up to the kW regime and to broadband driving lasers. Furthermore, the high tuning speed of this approach could be further increased by realizing the delay e.g. with a piezo driven mirror, making it attractive for the generation of quasi-supercontinua [13], thus benefitting applications such as XUV Coherence Tomography [38]. By implementing an electro-optical modulator even pulse-to pulse tuning appears feasible.

Funding. Daimler und Benz Stiftung (32-02/17); Carl-Zeiss-Stiftung; Deutsche Forschungsgemeinschaft (IRTG2101); Fraunhofer-Gesellschaft (Advanced Photon Sources); European Research Council (835306, SALT); Bundesministerium für Bildung und Forschung (05P19SJFAA, 05P2015); Thüringer Ministerium für Bildung, Wissenschaft und Kultur (2017 FGR 0076); European Social Fund; GSI Helmholtzzentrum für Schwerionenforschung (13N12082, Licht-Materie Wechselwirkung m. hochgelad. Ionen); Helmholtz Association (ECRAPS, Innovation Pool of the Research Field Matter).

Disclosures. M.T. is employed by Active Fiber Systems who distributes commercial XUV sources.

Optics EXPRESS

Data availability. Data underlying the results presented in this paper are not publicly available at this time but may be obtained from the authors upon reasonable request.

References

1. P. B. Corkum and F. Krausz, "Attosecond science," Nat. Phys. **3**(6), 381–387 (2007).
2. J. Rothhardt, G. K. Tadesse, W. Eschen, and J. Limpert, "Table-top nanoscale coherent imaging with XUV light," J. Opt. **20**(11), 113001 (2018).
3. A. L'Huillier, D. Descamps, A. Johansson, J. Norin, J. Mauritsson, and C.-G. Wahlström, "Applications of high-order harmonics," Eur. Phys. J. D - At. Mol. Opt. Phys. **26**(1), 91–98 (2003).
4. A. Cingöz, D. C. Yost, T. K. Allison, A. Ruehl, M. E. Fermann, I. Hartl, and J. Ye, "Direct frequency comb spectroscopy in the extreme ultraviolet," Nature **482**(7383), 68–71 (2012).
5. J. Rothhardt, S. Hädrich, S. Demmler, M. Krebs, D. F. A. Winters, T. Kühl, T. Stöhlker, J. Limpert, and A. Tünnermann, "Prospects for laser spectroscopy of highly charged ions with high-harmonic XUV and soft x-ray sources," Phys. Scr. **T166**, 014030 (2015).
6. J. W. Smith and R. J. Saykally, "Soft X-ray Absorption Spectroscopy of Liquids and Solutions," Chem. Rev. **117**(23), 13909–13934 (2017).
7. A. Trabattoni, L. Colaizzi, L. Ban, V. Wanie, K. Saraswathula, E. P. Månsson, P. Rupp, Q. Liu, L. Seiffert, E. A. Herzig, A. Cartella, B. L. Yoder, F. Légaré, M. F. Kling, T. Fennel, R. Signorell, and F. Calegari, "Photoelectron spectroscopy of large water clusters ionized by an XUV comb," JPhys Photonics **2**(3), 035007 (2020).
8. S. D. Kelly, D. Hesterberg, and B. Ravel, "*Analysis of Soils and Minerals Using X-ray Absorption Spectroscopy*," in (John Wiley & Sons, Ltd, 2015), pp. 387–463.
9. D. Popmintchev, B. R. Galloway, M.-C. Chen, F. Dollar, C. A. Mancuso, A. Hankla, L. Miaja-Avila, G. O'Neil, J. M. Shaw, G. Fan, S. Ališauskas, G. Andriukaitis, T. Balčiunas, O. D. Mücke, A. Pugzlys, A. Baltuška, H. C. Kapteyn, T. Popmintchev, and M. M. Murnane, "Near- and Extended-Edge X-Ray-Absorption Fine-Structure Spectroscopy Using Ultrafast Coherent High-Order Harmonic Supercontinua," Phys. Rev. Lett. **120**(9), 093002 (2018).
10. J. Guo, "Soft x-ray spectroscopy study of nanoscale materials," Proc. SPIE **5929**, 59290 K (2005).
11. W. Ubachs, "Resonant ionization spectroscopy in the XUV spectral region," in *AIP Conference Proceedings* (AIP, 1995), 329(1), pp. 283–288.
12. B. K. Agarwal, "*Soft X-Ray Spectroscopy*," in (Springer, 1991), pp. 279–301.
13. M. Wünsche, S. Fuchs, S. Aull, J. Nathanael, M. Möller, C. Rödel, and G. G. Paulus, "Quasi-supercontinuum source in the extreme ultraviolet using multiple frequency combs from high-harmonic generation," Opt. Express **25**(6), 6936–6944 (2017).
14. D. A. Shapiro, Y.-S. Yu, T. Tyliszczak, J. Cabana, R. Celestre, W. Chao, K. Kaznatcheev, A. L. D. Kilcoyne, F. Maia, S. Marchesini, Y. S. Meng, T. Warwick, L. L. Yang, and H. A. Padmore, "Chemical composition mapping with nanometre resolution by soft X-ray microscopy," Nat. Photonics **8**(10), 765–769 (2014).
15. B. Zhang, D. F. Gardner, M. H. Seaberg, E. R. Shanblatt, C. L. Porter, R. Karl, C. A. Mancuso, H. C. Kapteyn, M. M. Murnane, and D. E. Adams, "Ptychographic hyperspectral spectromicroscopy with an extreme ultraviolet high harmonic comb," Opt. Express **24**(16), 18745–1854 (2016).
16. A. Rana, J. Zhang, M. Pham, A. Yuan, Y. H. Lo, H. Jiang, S. J. Osher, and J. Miao, "Potential of Attosecond Coherent Diffractive Imaging," Phys. Rev. Lett. **125**(8), 086101 (2020).
17. R. A. Dilanian, B. Chen, G. J. Williams, H. M. Quiney, K. A. Nugent, S. Teichmann, P. Hannaford, L. V. Dao, and A. G. Peele, "Diffractive imaging using a polychromatic high-harmonic generation soft-x-ray source," J. Appl. Phys. **106**(2), 023110 (2009).
18. B. Chen, R. A. Dilanian, S. Teichmann, B. Abbey, A. G. Peele, G. J. Williams, P. Hannaford, L. Van Dao, H. M. Quiney, and K. A. Nugent, "Multiple wavelength diffractive imaging," Phys. Rev. A **79**(2), 023809 (2009).
19. G. S. M. Jansen, D. Rudolf, L. Freisem, K. S. E. Eikema, and S. Witte, "Spatially resolved Fourier transform spectroscopy in the extreme ultraviolet," Optica **3**(10), 1122–1125 (2016).
20. S. Witte, V. T. Tenner, D. W. Noom, and K. S. Eikema, "Lensless diffractive imaging with ultra-broadband table-top sources: from infrared to extreme-ultraviolet wavelengths," Light: Sci. Appl. **3**(3), e163 (2014).
21. Y. Meng, C. Zhang, C. Marceau, A. Y. Naumov, P. B. Corkum, and D. M. Villeneuve, "Octave-spanning hyperspectral coherent diffractive imaging in the extreme ultraviolet range," Opt. Express **23**(22), 28960–2869 (2015).
22. H. Eichmann, S. Meyer, K. Riepl, C. Momma, and B. Wellegehausen, "Generation of short-pulse tunable xuv radiation by high-order frequency mixing," Phys. Rev. A **50**(4), R2834–R2836 (1994).
23. M. B. Gaarde, P. Antoine, A. Persson, B. Carré, A. L'Huillier, and C.-G. Wahlström, "High-order tunable sum and difference frequency mixing in the XUV region," J. Phys. B: At., Mol. Opt. Phys. **29**(5), L163–L168 (1996).
24. M. Bellini, "Generation of widely tunable harmonic pulses in the UV and VUV from a NIR optical parametric amplifier," Appl. Phys. B **70**(6), 773–776 (2000).
25. B. Shan, A. Cavalieri, and Z. Chang, "Tunable high harmonic generation with an optical parametric amplifier," Appl. Phys. B **74**(S1), s23–s26 (2002).
26. F. Tani, M. H. Frosz, J. C. Travers, and P. S. J. Russell, "Continuously wavelength-tunable high harmonic generation via soliton dynamics," Opt. Lett. **42**(9), 1768 (2017).

Optics EXPRESS

27. C. Altucci, R. Bruzzese, C. de Lisio, M. Nisoli, S. Stagira, S. De Silvestri, O. Svelto, A. Boscolo, P. Ceccherini, L. Poletto, G. Tondello, and P. Villoresi, "Tunable soft-x-ray radiation by high-order harmonic generation," Phys. Rev. A **61**(2), 021801 (1999).
28. J. Zhou, J. Peatross, M. M. Murnane, H. C. Kapteyn, and I. P. Christov, "Enhanced High-Harmonic Generation Using 25 fs Laser Pulses," Phys. Rev. Lett. **76**(5), 752–755 (1996).
29. H. T. Kim, D. G. Lee, K.-H. Hong, J.-H. Kim, I. W. Choi, and C. H. Nam, "Continuously tunable high-order harmonics from atoms in an intense femtosecond laser field," Phys. Rev. A **67**(5), 051801 (2003).
30. W. Holgado, C. Hernández-García, B. Alonso, M. Miranda, F. Silva, O. Varela, J. Hernández-Toro, L. Plaja, H. Crespo, and I. J. Sola, "Tunable high-harmonic generation by chromatic focusing of few-cycle laser pulses," Phys. Rev. A **95**(6), 063823 (2017).
31. D. H. Reitze, S. Kazamias, F. Weihe, G. Mullot, D. Douillet, F. Augé, O. Albert, V. Ramanathan, J. P. Chambaret, D. Hulin, and P. Balcou, "Enhancement of high-order harmonic generation at tuned wavelengths through adaptive control," Opt. Lett. **29**(1), 86–88 (2004).
32. C. Winterfeldt, C. Spielmann, and G. Gerber, "Colloquium : Optimal control of high-harmonic generation," Rev. Mod. Phys. **80**(1), 117–140 (2008).
33. V. Hilbert, M. Tschernajew, R. Klas, J. Limpert, and J. Rothhardt, "A compact, turnkey, narrow-bandwidth, tunable, and high-photon-flux extreme ultraviolet source," AIP Adv. **10**(4), 045227 (2020).
34. L. Gulyás Oldal, T. Csizmadia, P. Ye, N. G. Harshitha, A. Zaïr, S. Kahaly, K. Varjú, M. Füle, and B. Major, "Generation of high-order harmonics with tunable photon energy and spectral width using double pulses," Phys. Rev. A **102**(1), 013504 (2020).
35. S. Kazamias, S. Daboussi, O. Guilbaud, K. Cassou, D. Ros, B. Cros, and G. Maynard, "Pressure-induced phase matching in high-order harmonic generation," Phys. Rev. A **83**(6), 063405 (2011).
36. J. Rothhardt, M. Krebs, S. Hädrich, S. Demmler, J. Limpert, and A. Tünnermann, "Absorption-limited and phase-matched high harmonic generation in the tight focusing regime," New J. Phys. **16**(3), 033022 (2014).
37. O. Pronin, V. Pervak, E. Fill, J. Rauschenberger, F. Krausz, and A. Apolonski, "Ultrabroadband efficient intracavity XUV output coupler," Opt. Express **19**(11), 10232 (2011).
38. S. Fuchs, M. Wünsche, J. Nathanael, J. J. Abel, C. Rödel, J. Biedermann, J. Reinhard, U. Hübner, and G. G. Paulus, "Optical coherence tomography with nanoscale axial resolution using a laser-driven high-harmonic source," Optica **4**(8), 903–906 (2017).